

# Quantum Correlation in One-dimensional Extended Quantum Compass Model

Wen-Long You\*

*School of Physical Science and Technology, Soochow University,  
Suzhou, Jiangsu 215006, People's Republic of China*

(Dated: April 19, 2019)

We study the correlations in the one-dimensional extended quantum compass model in a transverse magnetic field. By exactly solving the Hamiltonian, we find that the quantum correlation of the ground state of one-dimensional quantum compass model is vanishing. We show that quantum discord can not only locate the quantum critical points, but also discern the orders of phase transitions. Furthermore, entanglement quantified by concurrence is also compared.

PACS numbers: 03.67.-a, 64.70.Tg, 75.10.Jm, 75.25.Dk

## I. INTRODUCTION

Recently, there has been a revived interest in the study of correlations in quantum systems. In the framework of quantum-classical dichotomy, the total correlations can be separated into a purely quantum part and a classical counterpart, and both quantum correlation and classical correlation are able to be quantified respectively. A quantitative understanding of the different types of correlations might aid the application of quantum manipulation [1]. Therefore, distinguishing classical and quantum correlations in quantum systems is of both fundamental and practical importance. Paradoxically, entanglement was considered to be the most suitable manifestation of the quantum correlation and the main resource that speedup quantum computers over their classical counterparts [2, 3]. The studies of quantum correlations in exactly solvable models has a long tradition. For instance, the open-system dynamics of correlations in the presence of effect of environment is explored based on exact description [4–6].

Let us consider a bipartite system described by the density operator  $\rho_{AB}$  shared by parts  $A$  and  $B$ , and if it can be written in the separable form  $\rho_{AB} = \sum_j p_j \rho_A^{(j)} \otimes \rho_B^{(j)}$ , such mixed bipartite state is termed disentangled. Though all the correlations therein are local, some separable quantum states still contain intrinsically quantum correlations [7]. In this sense, it seems entanglement is not always needed for quantum speed-ups [8]. Quantum discord (QD) was thus introduced to quantify non-classical correlations beyond entanglement paradigm in quantum states [9], and it has received an astonishingly amount of interest both theoretically and experimentally [10–14].

In the field of quantum information, for a bipartite system  $\rho_{AB}$ , the total mutual information is the relative entropy between  $\rho_{AB}$  and  $\rho_A \otimes \rho_B$ , which corresponds to the minimal rate of randomness that is required to

completely erase all the correlations in  $\rho_{AB}$ ,

$$I(\rho_{AB}) = S(\rho_A) + S(\rho_B) - S(\rho_{AB}), \quad (1)$$

with von Neumann entropy  $S(\rho) = -\text{Tr} \rho \log(\rho)$ . The quantum conditional entropy over a set of Von Neumann measurement  $B_k$  is defined by

$$S(\rho_{AB}|B_k) := \sum_k p_k S(\rho_k), \quad (2)$$

where the measurement-based conditional density operator  $\rho_k$  associated with the measurement result  $k$  is

$$\rho_k = \frac{1}{p_k} (I_A \otimes B_k) \rho_{AB} (I_A \otimes B_k), \quad (3)$$

in which  $I_A$  is the identity operator of the subsystem  $A$  and  $p_k = \text{tr}[(I_A \otimes B_k) \rho_{AB} (I_A \otimes B_k)]$ . Consequently, the associated quantum mutual information is given by

$$I(\rho_{AB}|B_k) = S(\rho_A) - S(\rho_{AB}|B_k). \quad (4)$$

The classical mutual correlation is defined as the superior of  $I(\rho_{AB}|B_k)$  over all possible sets of one-dimensional positive-operator-valued measure (POVM)  $B_k$ ,

$$C(\rho_{AB}) = \sup_{\{B_k\}} I(\rho_{AB}|B_k). \quad (5)$$

The QD is then given by the difference of mutual information  $I(\rho_{AB})$  and the classical correlation  $C(\rho_{AB})$ ,

$$D(\rho_{AB}) = I(\rho_{AB}) - C(\rho_{AB}). \quad (6)$$

Since the minimization taken over POVMs is a notorious problem, so far only a few analytical results are obtained, including the Bell-diagonal states [15, 16], rank-2 states [17], and Gaussian states [18, 19]. Numerical efforts should be desired for general states. The QD can be shown to be asymmetric and nonnegative [20], and it is invariant under local unitary transformations. The QD will vanish if and only if the state is classical, and it is implied that classical-only correlated quantum states are extremely rare [21].

The QD not only can discern classical and quantum correlations, but also can be used to establish relation

---

\*Email: wlyou@suda.edu.cn

to quantum phase transitions (QPTs) of many-body systems. Information on the locations and the orders of the QPTs can be obtained by consideration of the derivatives of the bipartite QD with respect to the coupling parameters [22], and has also been generalized to multipartite state [23, 24]. As we know, a QPT identifies any point of nonanalyticity in the ground-state (GS) energy of an infinite lattice system. The patterns in correlations of a many-body system suddenly change across the quantum critical point (QCP), and induce the non-analytic behavior of ground state  $|\Psi_0\rangle$ . The reduced density matrix (RDM)  $\rho_{ij} = \text{Tr}_{ij}|\Psi_0\rangle\langle\Psi_0|$  is obtained by taking a partial trace over all degrees of freedom except particles  $i$  and  $j$ . The information of QPT is encoded in the non-analyticity of the matrix elements. With the QD being calculated from the RDM, one deduces that a discontinuity in the QD implies a first-order QPT, and a singularity in the derivative of the QD implies a second-order QPT [25]. Hence, the quantum correlation can serve as a hallmark for the QPT in the many-body system. We would like to stress that the RDM comprises more accessible information than the information of QPT only.

In this respect, we will take advantage of QD to study one-dimensional (1D) extended quantum compass model (EQCM) in the transverse magnetic field. The main reason for focusing on this model is that it not only allow us to study second-order phase transitions, but also allow the investigation of first-order transitions. The rest of the paper is organized as follows. In Sec. II, we introduce the 1D EQCM in the transverse magnetic field, and exploit the exact solutions. In Sec. III we calculate two-qubit QD of 1D EQCM. We show that QD can not only diagnose various phase transitions, but also identify the character of the QPTs. Consequently, the zero temperature phase diagram of the model is mapped out. In Sec. IV, we recheck the entanglement in the 1D EQCM in terms of concurrence. Sec. V finally contains the comparison between the concurrence and the QD and a short summary.

## II. QUANTUM PHASE TRANSITION IN ONE-DIMENSIONAL EXTENDED QUANTUM COMPASS MODEL IN A TRANSVERSE FIELD

The Hamiltonian of 1D EQCM in an external transverse magnetic field is given by [26, 27]

$$H = \sum_{i=1}^{N'} [J_1 \sigma_{2i-1}^x \sigma_{2i}^x + J_2 \sigma_{2i-1}^y \sigma_{2i}^y + L_1 \sigma_{2i}^x \sigma_{2i+1}^x + L_2 \sigma_{2i}^y \sigma_{2i+1}^y + \frac{h}{2} (\sigma_{2i-1}^z + \sigma_{2i}^z)], \quad (7)$$

where  $\sigma_i^a$  ( $a = x, y, z$ ) is the Pauli operator at site  $i$ ,  $J_1$  and  $J_2$  ( $L_1$  and  $L_2$ ) are the strength of the nearest-neighbor interaction on the odd (even) bond, and  $h$  characterizes the intensity of the external field applied in the

$z$  direction.  $N = 2N'$  is the number of the sites. We assume cyclic boundary conditions, i.e., the  $(N+1)$ th site is identified with the first site. The Hamiltonian describes a structure of two spins inside a unit cell. The orbital-orbital interactions depend strongly on the bond between two neighboring lattice sites. The Hamiltonian (7) encompasses two other well-known spin models: it turns into transverse Ising chain for  $J_1 = L_1, J_2 = L_2 = 0$  and the XY chain in a transverse field for  $J_1 = L_1, J_2 = L_2$ .

The Hamiltonian (7) can be exactly diagonalized by following the standard procedures. The Jordan-Wigner transformation maps explicitly between spin operators and spinless fermion operators by [28, 29]

$$\begin{aligned} \sigma_j^+ &= \exp \left[ i\pi \sum_{i=1}^{j-1} c_i^\dagger c_i \right] c_j = \prod_{i=1}^{j-1} \sigma_i^z c_j, \\ \sigma_j^- &= \exp \left[ -i\pi \sum_{i=1}^{j-1} c_i^\dagger c_i \right] c_j^\dagger = \prod_{i=1}^{j-1} \sigma_i^z c_j^\dagger, \\ \sigma_j^z &= 1 - 2c_j^\dagger c_j. \end{aligned} \quad (8)$$

Next discrete Fourier transformation for plural spin sites is introduced by

$$c_{2j-1} = \frac{1}{\sqrt{N'}} \sum_k e^{-ikj} a_k, \quad c_{2j} = \frac{1}{\sqrt{N'}} \sum_k e^{-ikj} b_k, \quad (9)$$

with the discrete momentums as

$$k = \frac{n\pi}{N'}, \quad n = -(N'-1), -(N'-3), \dots, N'-1. \quad (10)$$

Finally, the diagonalized form is achieved by a four-dimensional Bogoliubov transformation with two kind of quasiparticles [27, 30],

$$H = \sum_k \left[ E_k^o (\gamma_k^{o\dagger} \gamma_k^o - \frac{1}{2}) + E_k^a (\gamma_k^{a\dagger} \gamma_k^a - \frac{1}{2}) \right], \quad (11)$$

where optical spectra  $E_k^o = \sqrt{\varsigma + \sqrt{\tau}}$  and acoustic spectra  $E_k^a = \sqrt{\varsigma - \sqrt{\tau}}$ . Here  $\varsigma = |\alpha_k|^2 + |\beta_k|^2$ ,  $\tau = (\alpha_k^* \beta_k + \alpha_k \beta_k^*)^2 + 4|\alpha_k|^2 h^2$ ,  $\alpha_k = (J_1 + J_2) + (L_1 + L_2)e^{ik}$ , and  $\beta_k = (J_1 - J_2) - (L_1 - L_2)e^{ik}$ . The ground state  $E_0$  is obtained,

$$E_0 = -\frac{1}{2} \sum_k (E_k^o + E_k^a). \quad (12)$$

It is easy to find that the energy gap of acoustic branch will close when  $h = 2\sqrt{(J_1 \pm L_2)(J_2 \pm L_1)}$ , and the non-analyticities of the ground state determine QCPs. In the absence of the transverse magnetic field, i.e.,  $h = 0$ , the critical lines correspond to  $J_1 = \pm L_2$  and  $J_2 = \pm L_1$ , respectively, which confirms the conclusion in Ref. [31].

## III. TWO-QUBIT QUANTUM DISCORD OF EXTENDED QUANTUM COMPASS MODEL

The QD is explored from the two-qubit RDM. In the representation spanned by the two-qubit product states

$\{|0\rangle_A \otimes |0\rangle_B, |0\rangle_A \otimes |1\rangle_B, |1\rangle_A \otimes |0\rangle_B, |1\rangle_A \otimes |1\rangle_B\}$ , where  $|0\rangle$  ( $|1\rangle$ ) denotes spin up (down) state, the two-site density matrix can be expressed as,

$$\rho_{ij} = \frac{1}{4} \sum_{a,a'=0}^3 \langle \sigma_i^a \sigma_j^{a'} \rangle \sigma_i^a \sigma_j^{a'}, \quad (13)$$

where  $\sigma_i^a$  are Pauli matrices  $\sigma_i^x$ ,  $\sigma_i^y$  and  $\sigma_i^z$  for  $a = 1$  to 3, and 2 by 2 unit matrix for  $a=0$ . The Hamiltonian has  $Z_2$  symmetry, namely, the invariance under parity transformation  $P = \otimes_i \sigma_i^z$ , and then correlation functions such as  $\langle \sigma_i^a \sigma_j^b \rangle$  ( $a = x, y$  and  $b = 0, z$ ) simultaneously vanish. Also,  $\langle \sigma_i^x \sigma_j^y \rangle$  ( $\langle \sigma_i^y \sigma_j^x \rangle$ ) is zero due to the imaginary character of  $\sigma_j^y$  ( $\sigma_i^x$ ). Therefore, the two-qubit density matrix reduces to a X-state ,

$$\rho_{ij} = \begin{pmatrix} u^+ & 0 & 0 & z^- \\ 0 & w_1 & z^+ & 0 \\ 0 & z^+ & w_2 & 0 \\ z^- & 0 & 0 & u^- \end{pmatrix}, \quad (14)$$

with

$$u^\pm = \frac{1}{4}(1 \pm 2\langle \sigma_i^z \rangle + \langle \sigma_i^z \sigma_j^z \rangle), \quad (15)$$

$$z^\pm = \frac{1}{4}(\langle \sigma_i^x \sigma_j^x \rangle \pm \langle \sigma_i^y \sigma_j^y \rangle), \quad (16)$$

$$\omega_1 = \omega_2 = \frac{1}{4}(1 - \langle \sigma_i^z \sigma_j^z \rangle). \quad (17)$$

The density matrix of single qubit is easily obtained by a partial trace over one of the two qubits,

$$\rho_i = \begin{pmatrix} \frac{1}{2}(1 + \langle \sigma_i^z \rangle) & 0 \\ 0 & \frac{1}{2}(1 - \langle \sigma_i^z \rangle) \end{pmatrix}. \quad (18)$$

Thus the total correlation is quantified by the quantum mutual information as

$$I(\rho_{ij}) = S(\rho_i) + S(\rho_j) - S(\rho_{ij}), \quad (19)$$

with  $S(\rho_i) = S(\rho_j) = -\sum_{m=0}^1 \{ [1 + (-1)^m \langle \sigma_i^z \rangle] / 2 \} \log_2 \{ [1 + (-1)^m \langle \sigma_i^z \rangle] / 2 \}$  and  $S(\rho_{ij}) = -\sum_{m=0}^1 \xi_m \log_2 \xi_m - \sum_{n=0}^1 \xi_n \log_2 \xi_n$ , where  $\xi_m = [1 + \langle \sigma_i^z \sigma_j^z \rangle + (-1)^m \sqrt{(\langle \sigma_i^x \sigma_j^x \rangle - \langle \sigma_i^y \sigma_j^y \rangle)^2 + 4\langle \sigma_i^z \rangle^2}] / 4$  and  $\xi_n = [1 - \langle \sigma_i^z \sigma_j^z \rangle + (-1)^n (\langle \sigma_i^x \sigma_j^x \rangle + \langle \sigma_i^y \sigma_j^y \rangle)] / 4$ . Since part  $B$  contains a single qubit, we can compute the classical correlation by extremizing Eq. (5) over a complete set of orthogonal projectors  $\{B_k = |\Theta_\kappa\rangle\langle\Theta_\kappa|, \kappa = \parallel, \perp\}$ , where  $\Theta_\parallel \equiv \cos(\theta/2)|0\rangle_B + e^{i\varphi} \sin(\theta/2)|1\rangle_B$  and  $\Theta_\perp \equiv e^{-i\varphi} \sin(\theta/2)|0\rangle_B - \cos(\theta/2)|1\rangle_B$  with  $0 \leq \theta \leq \pi$  and  $0 \leq \varphi < 2\pi$ . Extensive numerical analysis implies that the extremization is mostly achieved at  $\theta = \pi/2$ ,  $\phi = 0$  [32, 33], which is also confirmed in our numerical optimization. Accordingly, the classical correlation is expressed as

$$C(\rho_{ij}) = H_{\text{bin}}(p_1) - H_{\text{bin}}(p_2), \quad (20)$$

where  $H_{\text{bin}}(p) = -p \log(p) - (1-p) \log(1-p)$  is the binary entropy,  $p_1 = (1 + \langle \sigma_i^z \rangle) / 2$  and  $p_2 = (1 + \sqrt{[\max(|\langle \sigma_i^x \sigma_j^x \rangle|, |\langle \sigma_i^y \sigma_j^y \rangle|)]^2 + \langle \sigma_i^z \rangle^2}) / 2$ . Thus the quantum correlation is simply given by

$$D(\rho_{ij}) = I(\rho_{ij}) - C(\rho_{ij}). \quad (21)$$

The Eq.(20) has been verified in Werner state [15], 1D Ising model, XY model [34], and XXZ model [22, 32], even for finite temperature [34–36].

First, we consider the QPT in 1D XY model, i.e.,  $J_1 = L_1$ ,  $J_2 = L_2$ .  $\gamma = (J_1 - J_2) / (J_1 + J_2)$  denotes the anisotropy of the coupling. The phase diagram is shown in Fig. 1, which describes two distinct QPTs. The transverse magnetic field  $h$  drives a second-order transition from an antiferromagnetic ordered phase to a paramagnetic quantum-disordered phase, and the anisotropy critical line  $\gamma = 0$  is the boundary between a Néel state along the  $x$  direction and a Néel state along the  $y$  direction [37, 38]. The first derivative of the QD for the nearest-neighboring odd bond is displayed in Fig. 1. It is evident there are rapid changes of QD in the critical regions. The changing rate of the QD is most pronounced for critical line  $\gamma = 0$ . The diverging first derivative of QD suggests both transitions belong to second-order phase transitions. Finite size scaling shows that the peak will not increase with respect to lattice size.

Next, we consider the QPT in 1D compass model, i.e.,  $J_1 = L_2 = 0$ . The ground state of finite-size system is  $2^{N'-1}$  fold degenerate [39]. In the absence of magnetic field  $h = 0$ , we note that there is only classical correlation created between nearest neighbors. In this case,  $E_k^o = 2\sqrt{J_2^2 + L_1^2} + 2J_2 L_1 \cos k$ ,  $E_k^a = 0$ . The only correlation functions surviving are  $\mathcal{C}_{2i-1,2i}^y \equiv \langle \sigma_{2i-1}^y \sigma_{2i}^y \rangle$  and  $\mathcal{C}_{2i,2i+1}^x \equiv \langle \sigma_{2i}^x \sigma_{2i+1}^x \rangle$ . As a consequence, the density matrix becomes densities diagonal in the orthogonal product bases. In other words, they are equivalent up to local unitary operations to Bell-diagonal states [40],

$$\begin{aligned} \rho_{2i-1,2i} &= \frac{1}{4} \begin{pmatrix} 1 & 0 & 0 & -\mathcal{C}_{2i-1,2i}^y \\ 0 & 1 & \mathcal{C}_{2i-1,2i}^y & 0 \\ 0 & \mathcal{C}_{2i-1,2i}^y & 1 & 0 \\ -\mathcal{C}_{2i-1,2i}^y & 0 & 0 & 1 \end{pmatrix} \\ &= \sum_{j=1}^4 \lambda_j |\Psi_j\rangle\langle\Psi_j|, \end{aligned} \quad (22)$$

where  $|\Psi_i\rangle$  are four Bell states with  $|\Psi_1\rangle = (|00\rangle + |11\rangle) / \sqrt{2}$ ,  $|\Psi_2\rangle = (|01\rangle + |10\rangle) / \sqrt{2}$ ,  $|\Psi_3\rangle = (|01\rangle - |10\rangle) / \sqrt{2}$ ,  $|\Psi_4\rangle = (|00\rangle - |11\rangle) / \sqrt{2}$ , and  $\lambda_1 = \lambda_3 = (1 - \mathcal{C}_{2i-1,2i}^y) / 8$ ,  $\lambda_2 = \lambda_4 = (1 + \mathcal{C}_{2i-1,2i}^y) / 8$ . We can find that QD vanishes in case of maximum  $\lambda_i$  is less than 0.5 [23, 41], that is,  $D(\rho_{2i-1,2i}) = 0$ . Similarly, the quantum correlation between two qubits on even bonds is also equal to zero, i.e.,  $D(\rho_{2i,2i+1}) = 0$ . In a sense, 1D compass model behaves as classical system. The null QD is induced by the macroscopic degeneracy of the ground state due to the peculiar symmetry of the

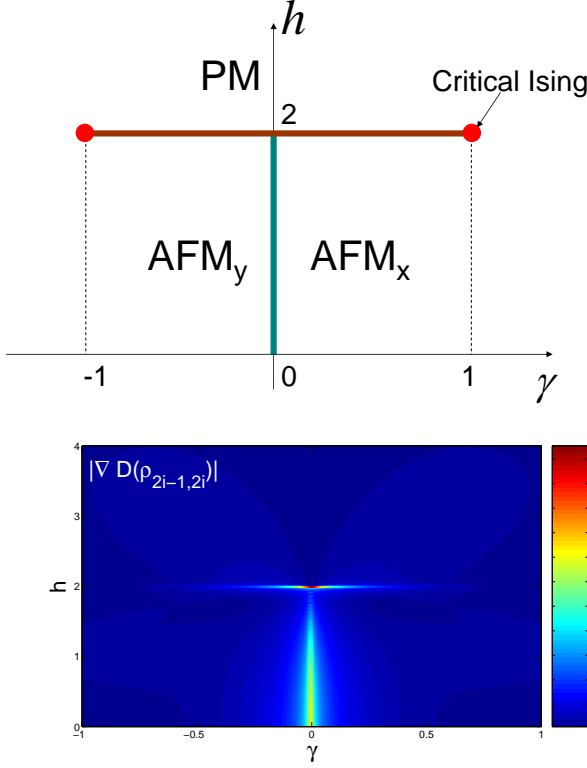


FIG. 1: (Color online) Top: phase diagram for the anisotropic XY spin-1/2 chain in a transverse field at zero temperature. The heavy lines represent second order phase transitions. The horizontal line will be referred to as the anisotropic transition and the vertical line as the Ising transition. PM denotes a paramagnetic phase and  $\text{AFM}_x$  ( $\text{AFM}_y$ ) denotes antiferromagnetic phase along the  $x$  ( $y$ ) direction. The XX model obtained by setting  $\gamma = 0$  displays a critical line for magnetic field  $h \in [0, 2]$ . The Ising model obtained for  $\gamma = 1$  exhibits a critical point at  $h = 2$ . Bottom: the first derivative of the QD between nearest neighbors in the  $\gamma - h$  plane.

Hamiltonian [42]. The similar strategy applies for the case  $J_2 = 0$ ,  $L_2 = 0$ ,  $h = 0$ . As a consequence, the energy spectra are greatly simplified as  $E_k^o = 2J_1$  and  $E_k^a = 2L_1$ . Then, the correlation functions are found to be  $\langle \sigma_{2i-1}^y \sigma_{2i}^y \rangle = \langle \sigma_{2i}^y \sigma_{2i+1}^y \rangle = 0$  and  $\langle \sigma_{2i-1}^x \sigma_{2i}^x \rangle = \langle \sigma_{2i}^x \sigma_{2i+1}^x \rangle = -1$ . In such case,  $D(\rho_{i,i+1}) = 0$ . We have verified that if a bipartite quantum state is a product state, i.e.,  $\rho_{AB} = \rho_A \otimes \rho_B$ , the state has no quantum correlations, not vice versa.

It has been shown that zero QD between a quantum system and its environment is necessary and sufficient for describing the evolution of the system through a completely positive map [43, 44]. In addition, a quantum state can be locally broadcast, i.e., of locally sharing preestablished correlations, if and only if it has zero QD [45, 46]. These purely classical states are rather unsteady, and a generic arbitrarily small perturbation will make them become nonclassical [21].

In the following, we will focus on the case of  $J_2 > 0$ ,

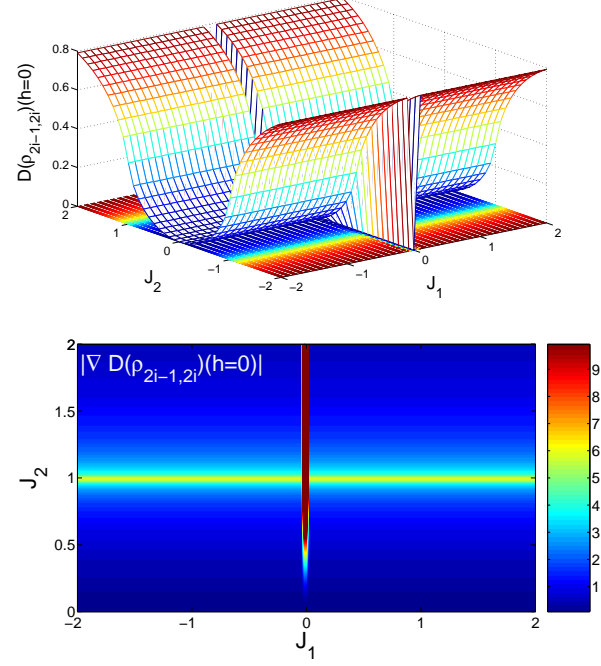


FIG. 2: (Color online) Top: QD of nearest-neighbor sites on odd bond as functions of  $J_1$  and  $J_2$  with parameters  $L_1 = 1$ ,  $L_2 = 0$ ,  $h = 0$ ,  $N = 1024$ . Bottom: the derivative of the QD in the  $J_1 - J_2$  plane.

$L_1 = 1$ . Minus sign of  $J_2$  is irrelevant because of unitary equivalence. In absence of external magnetic field, i.e.,  $h = 0$ , there is a first-order QPT at  $J_1 = 0$  which separates the phases with  $\langle \sigma_{2i-1}^x \sigma_{2i}^x \rangle = 1$  from those with  $\langle \sigma_{2i-1}^x \sigma_{2i}^x \rangle = -1$ . There is also a second-order QPT at  $J_2 = 1$  separating the phases with  $\langle \sigma_i^y \rangle = 0$  from those with  $\langle \sigma_i^y \rangle \neq 0$  [47]. Two critical lines where the energy gaps vanish, separate four gapped phases in the parameter space, as is shown in Fig. 2. Using Eqs. (19) - (21), the correlations can be evaluated in detail. We observe that QD indeed vanishes for  $J_1 = 0$ . The carmine contour line (very large values beyond the scope of colorbar) implies a first-order critical line while yellow contour line implies a second-order critical line. The occurrence of discontinuous dips at  $J_1 = 0$  implies a first-order critical line and a singularity of the first-order derivative of the QD reveals a second-order phase transition. To interpret the relation between the QD and QPTs more clearly, let us examine QPTs along three paths which start at the point  $J_1 = 1$ ,  $J_2 = 0$ , where Hamiltonian reduces to that of the 1D quantum Ising model. See Fig. 3 for an illustration.

In Fig. 4, we plot the QD verse  $J_1$  along the three paths shown in Fig. 3. It is clear that QD exhibits a sudden drop at  $J_1 = 0$ , suggesting a first-order QPT. For paths  $J_2 = (1 - J_1)/2$  and  $J_2 = 2(1 - J_1)$ , a diverging first derivative of QD signals a second-order QPT. As for the multicritical point on the line  $J_2 = 1 - J_1$ , a first-order

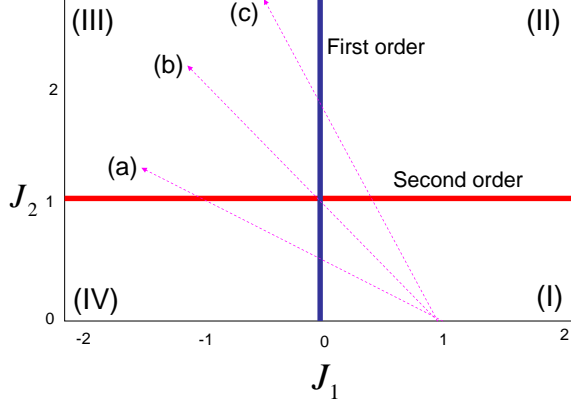


FIG. 3: (Color online) Phase diagram of the 1D quantum compass model in the absence of magnetic field. A first-order QPT occurs at critical line  $J_1 = 0$  and a second-order QPT at  $J_2 = 1$  [47]. We plot QD in Fig. (4) along three paths (a), (b), and (c) indicated by the dashed lines, which start at the point  $J_1=1, J_2=0$ , where the Hamiltonian (7) reduces to that of the one-dimensional quantum Ising model without external magnetic field.

phase transition dominates indicated by a discontinuity of the QD. Note that the classical correlation  $C(\rho_{ij}) = 1$  at  $J_1 \neq 0$ , and also has an abrupt decrease at  $J_1 = 0$ .

As mentioned above, the zero discord state is incredibly fragile, and finite perturbation can create QD. For example, the magnetic field will lift the high degeneracy of the 1D compass model. Therefore, we are especially interested in the role of the QD in detecting QPTs in 1D extended compass model under the magnetic field. In Fig. 5, we plot the QD of nearest-neighbor qubits as the function of  $J_1$  and  $J_2$  with external magnetic field. We present the contour map of the first derivative of the QD. With the increase of magnetic field  $h$ , we find that the critical lines deviate from those for  $h = 0$ , and the second-order critical line develops into hyperbolas.

Furthermore, we plot QD as a function of  $J_1$  along the path  $J_2 = J_1$  and its corresponding first-derivative for  $h = 2$  in Fig. 6. The divergent peaks show clearly that there will be QPTs at  $J_{1c} = (L_1 \pm \sqrt{L_1^2 + h^2})/2$  and  $(-L_1 \pm \sqrt{L_1^2 + h^2})/2$ , and these QPTs belong to second order. Hence, the phase diagram of 1D EQCM in the transverse magnetic field is sketched in Fig. 7, which is identical with that analyzed by correlation functions [30]. It is worthy noting that there are only continuous phase transitions once applying the magnetic field.

#### IV. ENTANGLEMENT

Given the exact solution of the 1D EQCM, we have a rare opportunity to analytically probe the entanglement in the ground state of a complex system. We here focus on one of the most frequently used entanglement mea-

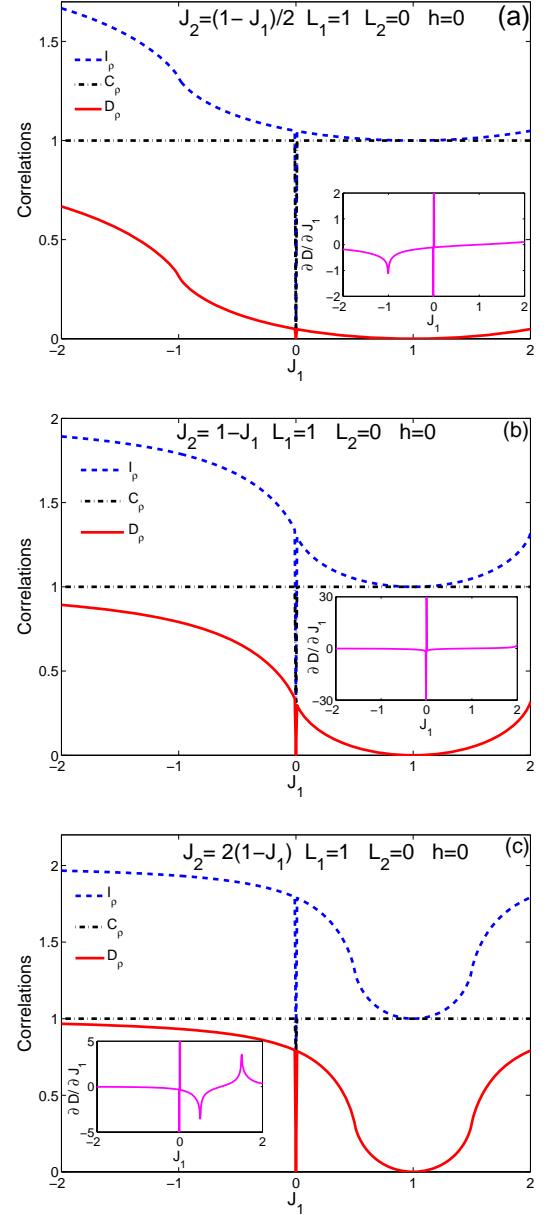


FIG. 4: (Color online) (a) The total mutual correlation, the classical correlation and quantum discord along the paths (a)  $J_2 = (1 - J_1)/2$  (b)  $J_2 = 1 - J_1$  (c)  $J_2 = 2(1 - J_1)$  shown in Fig. (3) with parameters  $L_1 = 1, L_2 = 0, N = 1024$ . The insets show the corresponding first derivative with respect to  $J_1$ . The diverging discontinuities have exceeded the  $y$ -limits of the coordinate axes.

sure: concurrence [48]. The concurrence can quantify entanglement for any bipartite system that relates to the two-site RMD  $\rho_{ij}$ , which is defined as

$$C(\rho_{ij}) = \max\{0, \lambda_1 - \lambda_2 - \lambda_3 - \lambda_4\}, \quad (23)$$

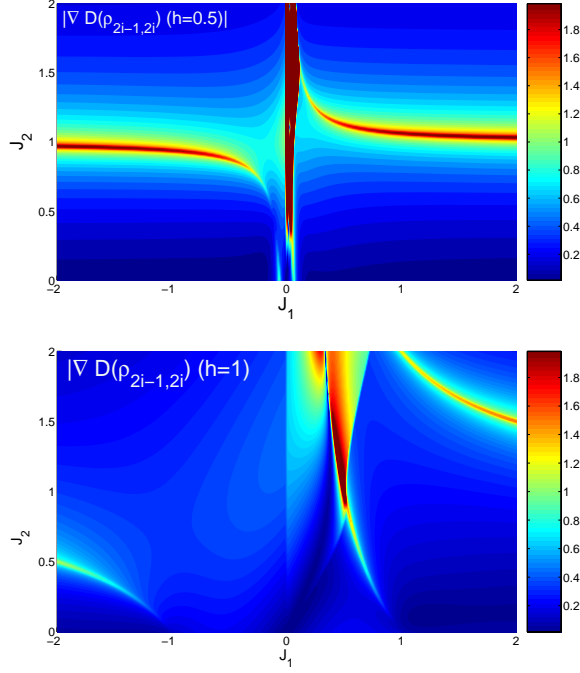


FIG. 5: (Color online) The derivative of the QD in the  $J_1 - J_2$  plane when  $L_1 = 1, L_2 = 0, N = 1024$  for magnetic field  $h = 0.5$  and  $h = 1$  respectively.

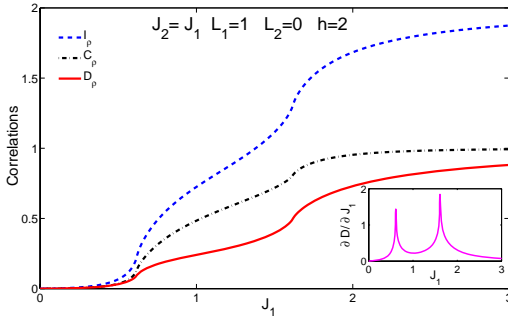


FIG. 6: (Color online) The total mutual correlation, the classical correlation and quantum discord along the path  $J_2 = J_1$  when  $L_1 = 1, L_2 = 0, L = 2048$  for magnetic field  $h = 2$ . The inset shows its first derivative.

where  $\lambda_i$  are the eigenvalues in decreasing order of the auxiliary matrix

$$\zeta = \sqrt{\rho_{ij}(\sigma_i^y \sigma_j^y) \rho_{ij}^* (\sigma_i^y \sigma_j^y)}. \quad (24)$$

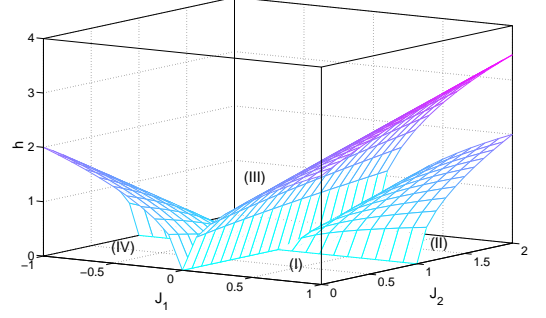


FIG. 7: (Color online) The phase diagram of the extended compass model in the transverse magnetic field,  $L_1 = 1, L_2 = 0$ . (I) spin-flop phase for  $J_1 > 0, J_2 < 1$ ; (II) antiparallel ordered of spin  $y$  component for  $J_1 > 0, J_2 > 1$ ; (III) saturated ferromagnetic phase for  $J_1 < 0, J_2 > 1$ ; (IV) stripe antiferromagnetic phase for  $J_1 < 0, J_2 < 1$ .

Here  $\rho_{ij}^*$  denotes the complex conjugation of  $\rho_{ij}$  in the standard basis. The eigenvalues of  $\zeta$  are

$$\begin{aligned} \lambda_{1,2} &= \frac{1}{4} \sqrt{1 + \langle \sigma_i^z \rangle + \langle \sigma_j^z \rangle + \langle \sigma_i^z \sigma_j^z \rangle} \\ &\quad \times \sqrt{1 - \langle \sigma_i^z \rangle - \langle \sigma_j^z \rangle + \langle \sigma_i^z \sigma_j^z \rangle \pm |\langle \sigma_i^x \sigma_j^x \rangle - \langle \sigma_i^y \sigma_j^y \rangle|}, \\ \lambda_{3,4} &= \frac{1}{4} \sqrt{1 + \langle \sigma_i^z \rangle - \langle \sigma_j^z \rangle - \langle \sigma_i^z \sigma_j^z \rangle} \\ &\quad \times \sqrt{1 - \langle \sigma_i^z \rangle + \langle \sigma_j^z \rangle - \langle \sigma_i^z \sigma_j^z \rangle \pm |\langle \sigma_i^x \sigma_j^x \rangle + \langle \sigma_i^y \sigma_j^y \rangle|}. \end{aligned} \quad (25)$$

For two spins that are on the same odd bond  $\{2i - 1, 2i\}$ , when  $J_1 > 0, L_1 = 1, L_2 = 0$ , the ground state resides in the subspace, where  $\langle \sigma_i^z \rangle = 0, \langle \sigma_{2i-1}^x \sigma_{2i}^x \rangle = -1, \langle \sigma_{2i-1}^y \sigma_{2i}^y \rangle = \langle \sigma_{2i-1}^z \sigma_{2i}^z \rangle$ , and then it is immediately clear that  $C(\rho_{ij}) = -\langle \sigma_{2i-1}^y \sigma_{2i}^y \rangle$ . On the other hand, when  $J_1 < 0$ , the ground state is in another subspace, where  $\langle \sigma_{2i-1}^y \sigma_{2i}^y \rangle = -\langle \sigma_{2i-1}^z \sigma_{2i}^z \rangle, \langle \sigma_{2i-1}^x \sigma_{2i}^x \rangle = 1$ , and then  $C(\rho_{ij}) = -\langle \sigma_{2i-1}^y \sigma_{2i}^y \rangle$ . However, at  $J_1 = 0, \langle \sigma_i^z \rangle = 0, \langle \sigma_{2i-1}^x \sigma_{2i}^x \rangle = 0, \langle \sigma_{2i-1}^y \sigma_{2i}^y \rangle = 0, \langle \sigma_{2i-1}^z \sigma_{2i}^z \rangle = 0$ , and then  $C(\rho_{ij}) = 0$ , which does not support the conjecture in Ref. [47] that the first-order QPT at  $J_1 = 0$  is not signaled by the pairwise concurrence. As is displayed in Fig. 8, the concurrence of nearest-neighbor pairs of spins captures the discontinuity across the first-order transition point when there is no external magnetic field, and the diverging peaks of the first derivative of concurrence imply the continuous QPTs.

## V. DISCUSSION AND CONCLUSION

Despite the resemblance in characterizing the QPTs in 1D EQCM, there still exist much difference between the concurrence and the QD. For example, the QD can present the correlations between neighbors farther than

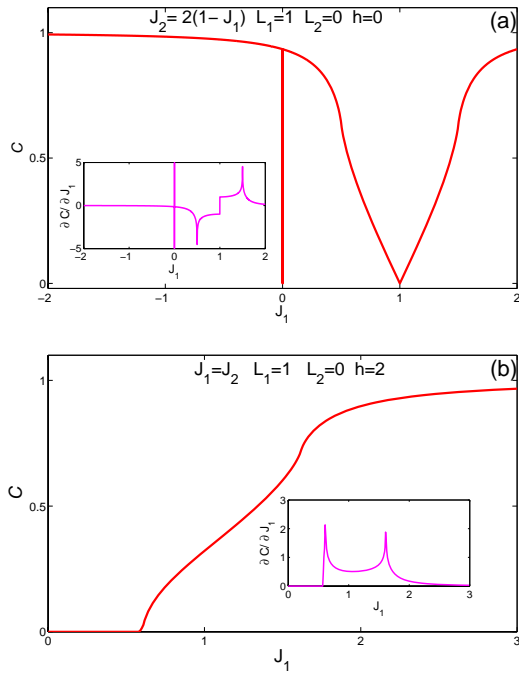


FIG. 8: (Color online) The concurrence of nearest neighbor spins on the odd bonds of with respect to  $J_1$  along path (a)  $J_2 = 2(1 - J_1)$  (b)  $J_2 = J_1$  with  $L_1 = 1, L_2 = 0, N = 1024$ . The corresponding first derivatives of concurrence are displayed in insets.

the next-nearest, while pairwise entanglement may be absent for these neighbors [34]. Besides, the QD can characterize QPTs by exhibiting long-range decay as a function of distance in spin systems, which is different from the behavior of pairwise entanglement [49]. Moreover, the thermal fluctuations extinguish the entanglement, while the QD is robust to spotlight QCPs at finite tempera-

ture [50]. The QD even increases with temperature in some cases [51]. Furthermore, there is an evidence that QD may present a scaling law, which is not the case for entanglement [52]. General speaking, quantum correlations are more fundamental than quantum entanglement, and may reveal more information about the quantum systems.

In conclusion, we have examined pairwise QD by exactly solving the 1D EQCM in the presence of an external transverse magnetic field. We find that the QD is equal to zero for the 1D compass model. Remarkably, we have successfully extracted information of the location and the order of the QPTs in 1D EQCM by consideration of the derivative of the QD with respect to the coupling parameters. We conclude that a first-order QPT is associated with a discontinuity in the QD and a continuous second-order transition demonstrates a diverging first derivative of QD. The mixed first-order and second-order phase transition point features a discontinuity. We get the analytic expressions of critical magnetic fields for the field-induced QPTs, which are of second order. As a result, we then obtain the phase diagram of 1D EQCM in the transverse magnetic field. For comparisons, we show that the pairwise concurrence can characterize the phase transitions by exhibiting similar behaviors. Nevertheless, the QD is believed to be more fundamental than concurrence in quantifying the quantum correlations, and should be of general interest in future studies.

## VI. ACKNOWLEDGEMENTS

Wen-Long You acknowledges the support of the Natural Science Foundation of Jiangsu Province under Grant No. 10KJB140010 and the National Natural Science Foundation of China under Grant No.11004144.

- 
- [1] L. Henderson and V. Vedral, J. Phys. A: Math. Gen. **34**, 6899 (2001)
  - [2] Luigi Amico, Rosario Fazio, Andreas Osterloh and Vlatko Vedral, Rev. Mod. Phys. **80**, 517 (2008)
  - [3] Ryszard Horodecki, Paweł Horodecki, Michał Horodecki, and Karol Horodecki, Rev. Mod. Phys. **81**, 865 (2009)
  - [4] Dajka, J. and Mierzejewski, M. and Luczka, J., Phys. Rev. A, **77**, 042316 (2011)
  - [5] Dajka, Jerzy and Luczka, Jerzy and Hänggi, Peter, Phys. Rev. A, **84**, 032120 (2011)
  - [6] W.L. You and Y.L. Dong, Eur. Phys. J. D **57**, 439 (2010)
  - [7] B. P. Lanyon, M. Barbieri, M. P. Almeida, and A. G. White, Phys. Rev. Lett. **101**, 200501 (2008)
  - [8] Animesh Datta, Anil Shaji, and Carlton M. Caves, Phys. Rev. Lett. **100**, 050502 (2008)
  - [9] H. Ollivier and W. H. Zurek, Phys. Rev. Lett. **88**, 017901 (2001)
  - [10] D. O. Soares-Pinto, L. C. Céleri, R. Auccaise, F. F. Fan-  
chini, E. R. deAzevedo, J. Maziero, T. J. Bonagamba, and R. M. Serra, Phys. Rev. A **81**, 062118 (2010)
  - [11] Jin-Shi Xu, Xiao-Ye Xu, Chuan-Feng Li, Cheng-Jie Zhang, Xu-Bo Zou, Guang-Can Guo, Nat. Commun. **1**, 7 (2010)
  - [12] Mazhar Ali, A. R. P. Rau, and G. Alber, Phys. Rev. A **81**, 042105 (2010)
  - [13] R. Auccaise, J. Maziero, L. C. Céleri, D. O. Soares-Pinto, E. R. deAzevedo, T. J. Bonagamba, R. S. Sarthour, I. S. Oliveira, and R. M. Serra, Phys. Rev. Lett. **107**, 070501 (2011)
  - [14] Kavan Modi, Aharon Brodutch, Hugo Cable, Tomasz Paterek, and Vlatko Vedral, arXiv:1112.6238 (unpublished)
  - [15] Shunlong Luo, Phys. Rev. A **77**, 042303 (2008)
  - [16] Matthias D. Lang and Carlton M. Caves, Phys. Rev. Lett. **105**, 150501 (2010)
  - [17] Li-Xiang Cen, Xin-Qi Li, Jiushu Shao and YiJing Yan, Phys. Rev. A **83**, 054101 (2011)

- [18] Gerardo Adesso and Animesh Datta, Phys. Rev. Lett. **105**, 030501 (2010)
- [19] Paolo Giorda and Matteo G. A. Paris, Phys. Rev. Lett. **105**, 020503 (2010)
- [20] W. H. Zurek, Rev. Mod. Phys. **75**, 715 (2003)
- [21] A. Ferraro, L. Aolita, D. Cavalcanti, F. M. Cucchietti, and A. Acín, Phys. Rev. A **81**, 052318 (2010)
- [22] Raoul Dillenschneider, Phys. Rev. B **78**, 224413 (2008).
- [23] Kavan Modi, Tomasz Paterek, Wonmin Son, Vlatko Vedral, and Mark Williamson, Phys. Rev. Lett. **104**, 080501 (2010).
- [24] P. Parashar and S. Rana, Phys. Rev. A **83**, 032301 (2011)
- [25] L.-A. Wu, M. S. Sarandy, and D. A. Lidar, Phys. Rev. Lett. **93**, 250404 (2004)
- [26] W. Brzezicki, J. Dziarmaga, and A. M. Oleś, Phys. Rev. B **75**, 134415 (2007).
- [27] W. Brzezicki, and A. M. Oleś, Acta Phys. Pol. A **115**, 162 (2009)
- [28] P. Jordan and E. Wigner, Z. Phys. **47**, 631 (1928)
- [29] S. Sachdev, *Quantum Phase Transitions*, (Cambridge University Press, Cambridge, UK, 2000)
- [30] R. Jafari, Phys. Rev. B **84**, 035112 (2011); arXiv:1105.0809 (unpublished)
- [31] Ke-Wei Sun and Qing-Hu Chen, Phys. Rev. B **80**, 174417 (2009)
- [32] M. S. Sarandy, Phys. Rev. A **80**, 022108 (2009)
- [33] Lu, X.-M., J. Ma, Z. Xi, and X. Wang, Phys. Rev. A **83**, 012327 (2011)
- [34] J. Maziero, H. C. Guzman, L. C. Céleri, M. S. Sarandy, and R. M. Serra, Phys. Rev. A **82**, 012106 (2010)
- [35] T. Werlang, C. Trippe, G. A. P. Ribeiro, and Gustavo Rigolin, Phys. Rev. Lett. **105**, 095702 (2010)
- [36] T. Werlang, G. A. P. Ribeiro, and Gustavo Rigolin, Phys. Rev. A **83**, 062334 (2011)
- [37] N. T. Jacobson, Silvano Garnerone, Stephan Haas, and Paolo Zanardi, Phys. Rev. B **79**, 184427 (2009)
- [38] J. E. Bunder and Ross H. McKenzie, Phys. Rev. B **60**, 344 (1999)
- [39] Wen-Long You and Guang-Shan Tian, Phys. Rev. B **78**, 184406 (2008)
- [40] L. Ciliberti, R. Rossignoli, and N. Canosa, Phys. Rev. A **82**, 042316 (2010)
- [41] Jie-Hui Huang, Lei Wang and Shi-Yao Zhu, New Journal of Physics **13**, 063045 (2011)
- [42] W. Brzezicki and A. M. Olés, Phys. Rev. B **82**, 060401 (2010)
- [43] A. Shabani and D. A. Lidar, Phys. Rev. Lett. **102**, 100402 (2009)
- [44] C. A. Rodriguez-Rosario, K. Modi, A. Kuah, A. Shaji, E. C. G. Sudarshan, J. Phys. A: Math. Gen. **41**, 205301 (2008)
- [45] Marco Piani, Paweł Horodecki, and Ryszard Horodecki, Phys. Rev. Lett. **100**, 090502 (2008)
- [46] H. Barnum, C. M. Caves, C. A. Fuchs, R. Jozsa and B. Schumacher, Phys. Rev. Lett. **76**, 2818 (1996)
- [47] Erik Eriksson and Henrik Johannesson, Phys. Rev. B **79**, 224424 (2009)
- [48] W. K. Wootters, Phys. Rev. Lett. **80**, 2245 (1998)
- [49] J. Maziero, L. C. Céleri, R. M. Serra and M. S. Sarandy, arXiv:1012.5926 (unpublished)
- [50] L. Mazzola, J. Piilo, and S. Maniscalco, Phys. Rev. Lett. **104**, 200401 (2010)
- [51] T. Werlang, G. Rigolin, Phys. Rev. A, **81**, 044101 (2010)
- [52] B. Tomasello, D. Rossini, A. Hamma, and L. Amico, Europhys. Lett. **96**, 27002 (2011)